Biomass-Derived Platform Chemicals: Thermodynamic Studies on the Conversion of 5-Hydroxymethylfurfural into Bulk Intermediates

Sergey P. Verevkin,* Vladimir N. Emel'yanenko, Elena N. Stepurko, Richardas V. Ralys, and Dmitry H. Zaitsau

Department of Physical Chemistry, University of Rostock, Dr-Lorenz-Weg 1, 18059 Rostock, Germany

Annegret Stark

Institute for Technical Chemistry and Environmental Chemistry, Friedrich-Schiller-University Jena, Lessingstrasse 12, 07743 Jena, Germany

This work was undertaken to obtain new thermochemical data for 5-hydroxymethylfurfural (HMF) and parent compounds. The standard molar enthalpy of formation in the gaseous state of HMF was obtained from combustion calorimetry, differential scanning calorimetry (DSC), and measurements of the temperature dependence of the vapor pressure by the transpiration method. To verify the experimental data, ab initio calculations of all compounds were performed. Enthalpies of formation derived from the G3MP2 method are in an excellent agreement with the experimental results. A weak hydrogen bond in HMF was revealed using ab initio methods. Thermodynamic analysis of the transformation of HMF to the bulk intermediates according to hydrogenation and oxidation pathways has revealed a very high feasibility of these reactions, with equilibrium constants that are completely shifted to the desired reaction products even at 298 K.

1. Introduction

Growing concerns about global warming indicate that sustainable and renewable sources of energy are needed in the near future. Ethanol, the only sugar-based renewable liquid fuel currently produced in large quantities, suffers from several limitations, including low energy content and high volatility. Cellulose and other carbohydrates (e.g., glucose and fructose) can be converted into furanic biofuels via 5-hydroxymethylfurfural (HMF), using relatively simple processes such as condensation and hydrogenation reactions. Furanic ethers, esters, or 2,5-dimethylfuran produced in this way have been described as fuel additives.[1–3] Compared to ethanol, 2,5-dimethylfuran has a higher energy density,[4] has a higher boiling point (by 20 °C), and is not soluble in water. Hence, the development of strategies for transforming abundant renewable biomass into a liquid fuel suitable for the transportation sector could diminish the reliance on petroleum.

In the past several years, tremendous progress in the effective production of HMF has been achieved by allowing for the use of glucose-containing starting material in its manufacture. The simple Brønsted-acid catalysis studied previously allowed only for the conversion of the more expensive and less abundant fructose. To date, it has been demonstrated that the in situ isomerization of glucose to fructose with subsequent condensation to HMF is feasible in high yields (70−80%)[4–6] using Lewis-acid catalysts such as $CrCl_2$ and ionic liquids as solvents,[5] paving the way to the use of abundant raw feedstock (wheat straw, cellulose, wood, etc.).[4,7]

Although the introduction of sugar-based materials into industrial applications is presently still in its infancy for reasons such as the lack of knowledge of their detailed physicochemical properties, the noncompetitiveness of the price compared to petrol-based chemicals, and the existence of only a few established industrial processes, several promising building blocks have been prepared from multifunctional HMF,[8–11] highlighting the potential for replacing petrol-based feedstock. Examples of possible market segments are found in applications as solvents, monomers, coatings, adhesives, and sealants, as well as fine-chemical or pharmaceutical intermediates.

With the goal of enhancing the knowledge about the thermochemical properties of HMF and some of its oxidized and hydrogenated products, some major synthetic directions toward biofuels and chemical building blocks were investigated to build an extended and reliable physicochemical database on a wide variety of new organic compounds. In this work, the primary attention was paid to obtain thermodynamic properties of 5-hydroxymethylfurfural. The molar enthalpy of formation of solid HMF was measured using combustion calorimetry. The molar enthalpy of vaporization of HMF was obtained from the temperature dependence of the vapor pressure measured by the transpiration method. The molar enthalpy of fusion of HMF was measured by differential scanning calorimetry (DSC). Ab initio calculations of the gaseous molar enthalpy of formation of HMF were performed using the G3MP2 method, and the results are in good agreement with the experimental data.

To study the feasibility of producing basic chemical building blocks by the conversion of HMF, the thermodynamics of the hydrogenation and oxidation reactions were systematically studied in this work using composite G*-family and density functional theory (DFT) methods. Thermodynamic analysis of the transformation of HMF to the bulk intermediates according to hydrogenation and oxidation pathways (Figure 1) has revealed a very high feasibility of these reactions, with the equilibrium constants completely shifted to the desired reaction products even at 298 K.

2. Experimental Section

2.1. Materials. The sample of 5-hydroxymethylfurfural [CAS 67-47-0] was of commercial origin (Aldrich), having a mass-fraction purity of about 0.99, and was purified by repeated

* To whom correspondence should be addressed. E-mail: sergey.verevkin@uni-rostock.de.

10.1021/ie901012g CCC: $40.75
Published on Web 09/11/2009

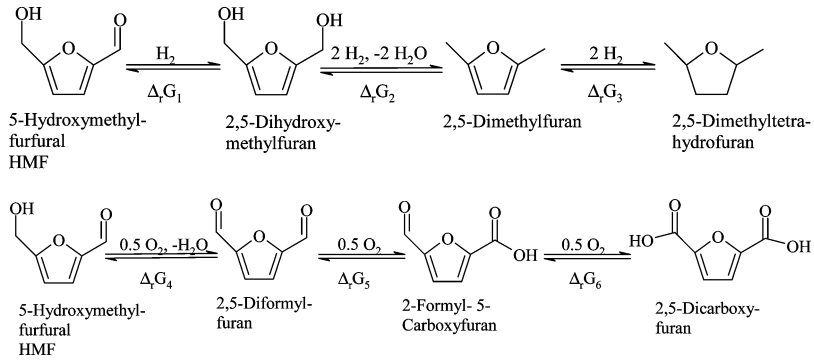

Figure 1. Hydrogenation reactions of HMF to 2,5-dihydroxymethylfuran (R1), 2,5-dimethylfuran (R2), and 2,5-dimethyltetrahydrofuran (R3) and oxidation reactions of HMF to 2,5-diformylfuran (R4), 2-formyl-5-carboxyfuran (R5), and 2,5-dicarboxyfuran (R6).

sublimation in vacuum. The degree of purity (better than 99.9%) was determined using a Hewlett-Packard 5890 Series II gas chromatograph equipped with a flame ionization detector and a Hewlett-Packard 3390A integrator. The flow of the carrier gas (nitrogen) was 7.2 $dm^3 \cdot h^{-1}$. An HP-5 capillary column (stationary phase of cross-linked 5% PH ME silicone) with a column length of 30 m, an inside diameter of 0.32 mm, and a film thickness of 0.25 μm was used. The standard temperature program of the gas chromatograph (GC) was $T = 303$ K for 180 s, followed by a heating rate of 10 $K \cdot min^{-1}$ to $T = 523$ K.

2.2. Vapor Pressure Measurements of HMF. Transpiration Method. Vapor pressures over a liquid sample of HMF were determined using the method of transpiration in a saturated nitrogen flow. The method has been described before[12,13] and has proven to give results that are in excellent agreement with other established techniques for determining vapor pressures of pure substances in the range of 0.005 to approximately 10000 Pa and enthalpies of vaporization from the temperature dependence of the vapor pressure. About 0.5 g of the sample was mixed with glass beads and placed in a thermostatted U-shaped tube having a length of 20 cm and a diameter of 0.5 cm. Glass beads with a diameter of 1 mm provide a surface area large enough for rapid vapor−liquid equilibration. At constant temperature (±0.1 K), a nitrogen flow was passed through the U-tube, and the transported amount of gaseous material was collected in a cold trap. The flow rate of nitrogen was measured using a soap-bubble flow meter and was optimized to reach the saturation equilibrium of the transporting gas at each temperature under study. The amount of condensed substance was determined by GC analysis using an external standard (*n*-nonane). The saturation vapor pressure p_i^{sat} at each temperature T was calculated from the amount of the product collected within a definite period of time. Assuming that Dalton's law of partial pressures applies to the nitrogen stream saturated with the substance i of interest, values of p_i^{sat} were calculated with the following equations, assuming ideal gas behavior

$$p_i^{sat} = m_i R T_a / V M_i, \quad V = V_{N_2} + V_i \quad (V_{N_2} \gg V_i) \qquad (1)$$

where $R = 8.314472$ $J \cdot K^{-1} \cdot mol^{-1}$, m_i is the mass of the transported compound, M_i is the molar mass of the compound, and V_i is its volume contribution to the gaseous phase. V_{N_2} is the volume of the carrier gas, and T_a is the temperature of the soap-bubble meter. The volume of the carrier gas, V_{N_2}, was determined from the flow rate and the time measurement. Results from the transpiration experiments are given in Table 1.

2.3. Combustion Calorimetry. An isoperibol bomb calorimeter was used for the measurement of the energy of combustion of HMF. In the present study, we used commercially available polyethene bulbs (NeoLab, Heidelberg, Germany) of 1 cm^3 volume as the sample containers. Results from combustion experiments are given in Table 2. The detailed procedure has been described previously.[14,15] The combustion products were examined for carbon monoxide (Dräger tube) and unburned carbon, but neither of these substances was detected. The energy equivalent of the calorimeter, ε_{calor}, was determined with a standard reference sample of benzoic acid (sample SRM 39i, NIST). Correction for nitric acid formation was based on titration with 0.1 $mol \cdot dm^{-3}$ NaOH (aqueous). The atomic weights used were those recommended by the IUPAC Com-

Table 1. Vapor Pressures, p, and Enthalpies of Vaporization, $\Delta_l^g H_m$, Obtained for 5-Hydroxymethylfurfural by the Transpiration Method

T^a (K)	m^b (mg)	$V(N_2)^c$ (dm^3)	flow ($dm^3 \cdot h^{-1}$)	$p^{d,e}$ (Pa)	$p_{exp} - p_{calc}$ (Pa)	$\Delta_l^g H_m{}^f$ ($kJ \cdot mol^{-1}$)
313.4	2.51	115.0	5.41	0.43	0.02	82.24
314.3	2.66	109.9	5.23	0.47	0.02	82.17
318.3	2.24	63.99	5.45	0.68	0.02	81.86
318.3	3.05	90.83	5.32	0.66	−0.01	81.86
321.3	2.02	44.20	3.80	0.89	0.00	81.63
323.2	1.19	22.00	5.50	1.08	0.02	81.48
326.2	0.95	13.20	10.70	1.40	−0.01	81.25
328.2	2.77	33.18	2.80	1.64	−0.05	81.09
328.2	0.51	6.16	5.20	1.62	−0.07	81.09
331.1	1.46	13.04	9.10	2.18	−0.02	80.86
333.1	0.52	3.97	5.17	2.56	−0.05	80.71
333.2	2.36	18.00	5.43	2.56	−0.08	80.70
335.1	1.44	8.95	9.10	3.15	0.02	80.55
338.2	0.84	4.13	1.69	3.96	−0.09	80.31
338.2	1.64	8.10	5.29	3.95	−0.11	80.31
341.1	1.11	4.24	9.09	5.10	−0.07	80.09
343.1	2.85	9.03	2.81	6.16	0.03	79.93
343.2	1.19	3.80	5.31	6.13	−0.01	79.92
345.1	2.20	5.74	9.06	7.46	0.29	79.78
346.1	3.17	7.78	2.83	7.96	0.19	79.70
347.1	1.29	3.03	9.08	8.29	−0.13	79.62
348.1	1.29	2.74	5.30	9.20	0.09	79.54
351.1	1.35	2.30	9.20	11.49	−0.03	79.31
353.1	3.47	5.01	5.37	13.52	0.09	79.15
355.1	2.01	2.46	9.23	15.90	0.27	79.00
358.1	3.76	3.83	5.47	19.11	−0.44	78.77
361.1	2.70	2.12	7.47	24.88	0.52	78.53
363.1	3.91	2.67	5.33	28.71	0.58	78.38
368.1	2.47	1.21	2.80	40.04	0.05	77.99

[a] Temperature of saturation. [b] Mass of transferred sample, condensed at $T = 243$ K. [c] Volume of nitrogen, used to transfer the mass m of sample. [d] Vapor pressure at temperature T, calculated from m and the residual vapor pressure at the cooling temperature $T = 243$ K. [e] Experimental data were fitted to the following equation:

$$\ln(p/\text{Pa}) = \frac{336.75}{R} - \frac{106621.75}{R(T/\text{K})} - \frac{77.8}{R} \ln\left(\frac{T/\text{K}}{298.15}\right).$$

[f] $\Delta_l^g H_m(298\text{ K}) = (83.43 \pm 0.24)$ $kJ \cdot mol^{-1}$.

Table 2. Results of Typical Combustion Experiments at $T = 298$ K ($p^\circ = 0.1$ MPa) for 5-Hydroxymethylfurfural[a]

	1	2	3	4	5
m(substance)[b] (g)	0.906069	0.603773	0.645379	0.706138	0.754693
m'(cotton)[b] (g)	0.000797	0.001073	0.000919	0.000995	0.000819
m''(polyethene)[b] (g)	0.273133	0.253858	0.208708	0.205023	0.221018
ΔT_c[c] (K)	2.20382	1.69637	1.61716	1.69637	1.81811
$\varepsilon_{calor}(-\Delta T_c)$ (J)	−32650.6	−25132.5	−23959	−25132.5	−26936.3
$\varepsilon_{cont}(-\Delta T_c)$ (J)	−37.46	−27.42	−25.93	−27.38	−29.79
$\Delta U_{decomp}(HNO_3)$ (J)	21.5	47.18	43.6	48.38	44.79
ΔU_{corr}[d] (J)	21.32	14.42	14.49	15.62	16.96
$-m'\Delta_c u'$ (J)	13.51	18.18	15.57	16.86	13.88
$-m''\Delta_c u''$ (J)	12660.15	11766.72	9673.95	9503.14	10244.54
$\Delta_c u^\circ$(liq) (J·g^{-1})[e]	−22042.0	−22050.4	−22060.4	−22057.9	−22056.5

[a] For the definition of the symbols, see ref 17. Calorimeter: T_h = 298.15 K, V(bomb) = 0.320 dm^3, p^i(gas) = 3.04 MPa, $m^i(H_2O)$ = 1.00 g. [b] Masses obtained from apparent masses. [c] $\Delta T_c = T^f - T^i + \Delta T_{corr}$; $\varepsilon_{cont}(-\Delta T_c) = \varepsilon^i_{cont}(T^i - 298.15\ K) + \varepsilon^f_{cont}(298.15\ K - T^f + \Delta T_{corr})$. [d] ΔU_{corr}, the correction to standard states, is the sum of items 81−85, 87−90, 93, and 94 in ref 17. [e] $\varepsilon = 14815.5 \pm 0.6$ J·K^{-1}. Water content of 412.08 ppm has been taken into account.

mission.[16] The sample masses were reduced to vacuum, taking into consideration their density values (see Table S1, Supporting Information). For conversion of the energy of the actual bomb process to that of the isothermal process and reduction to standard states, the conventional procedure[17] was applied. Small amounts of water could not be removed from the samples prepared for thermochemical measurements. The exact amount of water (412.1 ppm) in the sample for the combustion experiments was measured by Karl Fischer titration, and the appropriate corrections to the masses of samples were performed.

2.4. Phase Transitions in the Solid State. DSC Measurements. Information about the possible phase transitions in the sample under study is indispensable for vapor-pressure measurements using the transpiration method. Such knowledge helps in the choice of the temperature range for investigation and allows for vapor-pressure measurements within the range where the compound of interest exists in only a certain crystalline modification. For this reason, crystalline samples are usually studied by DSC prior to transpiration experiments. The thermal behavior of HMF, including melting temperature and enthalpy of fusion, was determined with a computer-controlled Perkin-Elmer Pyris Diamond differential scanning calorimeter. For all measurements, an empty pan was used as the reference. The fusion temperature and enthalpy were determined as the peak onset temperature and by using a straight baseline for integration, respectively. The temperature and heat-flow-rate scale of the DSC were calibrated by measuring high-purity indium (T_0 = 429.8 K and ΔH_{ref} = 28.4 J·g^{-1}). The thermal behavior of the specimen was investigated at a heating rate of 10 K·min^{-1}. The uncertainty in temperature was ±0.5 K, and that in the enthalpy of fusion was ±1 J·g^{-1}. The DSC measurements on the sample of HMF were repeated five times and values agreed to within the experimental uncertainties: ±0.4 kJ·mol^{-1} for the enthalpy of fusion and ±0.5 K for the melting temperature.

2.5. Computations. Standard ab initio molecular orbital calculations were performed with the Gaussian 03, rev. 04, series of programs.[18] Energies were obtained at the DFT [B3LYP/6-311++G(3df,3pd)] and G3MP2 levels of theory. G3 theory is a procedure for calculating the energies of molecules containing atoms of the first and second rows of the periodic table based on ab initio molecular orbital theory. A modification of G3 theory that uses reduced orders of Møller−Plesset perturbation theory is G3MP2 theory.[19] No corrections for internal rotors were taken into account. The enthalpy values at $T = 298$ K were evaluated according to standard thermodynamic procedures.[20]

3. Results and Discussion

The enthalpy of formation in the gas phase, $\Delta_f H^\circ_m(g)$, of any compound is made up of three contributions

$$\Delta_f H^\circ_m(g) = \Delta_f H^\circ_m(cr) + \Delta^g_l H_m + \Delta^l_{cr} H_m \quad (2)$$

where $\Delta_f H^\circ_m(cr)$ is the enthalpy of formation in the solid state, $\Delta^g_l H_m$ is the enthalpy of vaporization, and $\Delta^l_{cr} H_m$ is the enthalpy of fusion. Experimental determinations of $\Delta_f H^\circ_m(cr)$, $\Delta^g_l H_m$, and $\Delta^l_{cr} H_m$ of HMF are discussed below.

3.1. Vapor Pressures and Vaporization Enthalpy of HMF. Experimental vapor pressures of HMF measured in this work and the enthalpy of vaporization (Table 1) were treated with eqs 3 and 4, respectively

$$R \ln p_i^{sat} = a + \frac{b}{T} + \Delta^g_l C_p \ln\left(\frac{T}{T_0}\right) \quad (3)$$

$$\Delta^g_l H_m(T) = -b + \Delta^g_l C_p T \quad (4)$$

where p_i^{sat} is the vapor pressure, a and b are adjustable parameters (Table 1), T_0 is an arbitrarily chosen reference temperature (T_0 is 298.15 K in this work), and $\Delta^g_l C_p = 77.8$ J·mol^{-1}·K^{-1} is the difference of the molar heat capacities of the gaseous and the liquid phases (C^l_p). Values of $C^l_p = 258.5$ J·mol^{-1}·K^{-1} and $\Delta^g_l C_p = 77.8$ J·mol^{-1}·K^{-1} were calculated using the group contribution method of Chickos and Acree.[21] To assess the uncertainty in the vaporization enthalpy, the experimental data were approximated with the linear equation $\ln(p_i^{sat}) = f(T^{-1})$ using the least-squares method. The uncertainty in the enthalpy of vaporization was assumed to be identical to the average deviation of experimental $\ln(p_i^{sat})$ values from this linear correlation, and uncertainties in values of $\Delta^g_l C_p$ were not taken into account. We checked the experimental and calculation procedure with measurements of vapor pressures of *n*-alkanols.[12] It turned out that vapor pressures derived from the transpiration method were reliable to within 1−3% and their accuracy was governed by the reproducibility of the GC analysis.

3.2. Energy of Combustion and Enthalpy of Formation of HMF. Results of combustion experiments on HMF are given in Table 2. The value of the standard specific energy of combustion, $\Delta_c u^\circ = -(22053.4 \pm 3.3)$ J·g^{-1}, was used to derive the standard molar enthalpy of combustion, $\Delta_c H^\circ_m(cr) = -(2781.2 \pm 1.0)$ kJ·mol^{-1}, and the standard molar enthalpy of formation in the solid state, $\Delta_f H^\circ_m(cr) = -(437.4 \pm 1.3)$ kJ·mol^{-1}, based on the reaction

$$C_6H_6O_6 + 6O_2 = 6CO_2 + 3H_2O \quad (5)$$

$\Delta_f H^\circ_m(cr)$ of HMF was obtained from the enthalpic balance according to the equation

$$\Delta_f H^\circ_m(cr, C_6H_6O_3) = 6\Delta_f H^\circ_m(g, CO_2) + 3\Delta_f H^\circ_m(l, H_2O) - \Delta_c H^\circ_m(cr, C_6H_6O_3) \quad (6)$$

where the molar enthalpies of formation of H_2O(l) and CO_2(g) were taken from the literature, as recommended by CODATA.[22] The uncertainty assigned to $\Delta_f H^\circ_m(cr)$ is twice the overall standard deviation and includes the uncertainties from calibration, from the combustion energies of the auxiliary materials, and from the enthalpies of formation of the reaction products H_2O and CO_2. The enthalpy of combustion of HMF was reported as 2781.5 kJ·mol^{-1} 90 years ago.[23] This value was measured by bomb combustion calorimetry at 20 atm oxygen pressure. Despite the wrong algebraic sign, the older value is surprisingly

Table 3. Thermochemical Data at $T = 298$ K ($p^\circ = 0.1$ MPa) for 5-Hydroxymethylfurfural[a])

quantity	value	quantity	value
$\Delta_c H_m^\circ$(cr)	-2781.2 ± 1.0	$\Delta_f^g H_m$	83.4 ± 0.2
$\Delta_f H_m^\circ$(s)	-437.4 ± 1.3	$\Delta_f H_m^\circ(g)_{exp}$	-334.2 ± 1.4
$\Delta_{cr}^l H_m$	19.8 ± 0.4[b]	$\Delta_f H_m^\circ(g)_{G3MP2}$	-333.9 ± 2.3
$\Delta_{cr}^g H_m$	103.2 ± 0.5[c]		

[a] All values in kJ·mol^{-1}. [b] Experimental enthalpy of fusion $\Delta_{cr}^l H_m$ measured at T_{fus} and adjusted to 298 K (see text). [c] Obtained as the sum of $\Delta_{cr}^l H_m + \Delta_f^g H_m$ given in this table.

in an excellent agreement with the redetermination performed in this work: $\Delta_c H_m^\circ(cr) = -(2781.2 \pm 1.0)$ kJ·mol^{-1}.

3.3. Enthalpy of Fusion of HMF. The melting temperature and enthalpy of fusion for HMF were measured in the present work using DSC. The onset, peak, and end temperatures of the melting peak were 306.1, 308.5, and 312.1 K, respectively, and the enthalpy of fusion was found to be $\Delta_{cr}^l H_m = 19.8 \pm 0.4$ kJ·mol^{-1}. No phase transitions other than melting were detected. As a rule, all thermodynamic quantities in eq 2 should be referred to the same temperature, often $T = 298$ K. However, the experimental enthalpy of fusion of HMF measured by DSC was obtained at the melting temperature, T_{fus}. Because of the differences in the reference temperatures, the experimental enthalpies of fusion were adjusted to $T = 298$ K. The adjustment was calculated from the equation[12]

$$[\Delta_{cr}^l H_m(T_{fus}/\mathrm{K}) - \Delta_{cr}^l H_m(298\ \mathrm{K})]/(\mathrm{J \cdot mol^{-1}}) = \{(0.75 + 0.15 C_p^{cr})[(T_{fus}/\mathrm{K}) - 298\ \mathrm{K}]\} - \{(10.58 + 0.26 C_p^l)[(T_{fus}/\mathrm{K}) - 298\ \mathrm{K}]\} \quad (7)$$

where the isobaric molar heat capacities of solid and liquid HMF, $C_p^{cr} = 209.7$ J·mol^{-1}·K^{-1} and $C_p^l = 258.5$ J·mol^{-1}·K^{-1}, respectively, were calculated using the procedure of Chickos and Acree.[21] With this adjustment (the uncertainty of the correlation was not taken into account), the molar enthalpy of fusion, $\Delta_{cr}^l H_m$(298 K), of HMF was calculated (Table 3).

3.4. Calculation of the Gaseous Enthalpies of Formation of HMF. The value of the vaporization enthalpy of HMF derived in this work (Table 1) was used together with the results from combustion experiments (Table 2) and the fusion enthalpy (Table 3) for further calculation of the gaseous standard enthalpies of formation, $\Delta_f H_m^\circ(g)$, at 298 K according to eq 2. The resulting value of $\Delta_f H_m^\circ(g) = -(334.2 \pm 1.4)$ kJ·mol^{-1} for HMF is given in Table 3 (second-to-last entry).

3.5. Quantum Chemical Calculations. Results of ab initio molecular orbital methods for calculation of the enthalpy of formation of HMF have not been yet reported in the literature.

3.5.1. Conformational Equilibrium of HMF. Study of conformational equilibrium of HMF is important for the correct calculation of its enthalpy of formation, $\Delta_f H_m^\circ(g)$. According to conformational analysis using the G3MP2 method, seven possible arrangements of HMF were found. The most stable conformation of HMF is presented in Figure 2. The energy differences of the seven conformers of HMF related to the appropriate most stable conformer (index st) are given in Table S2 (Supporting Information). The thermal populations, p_i, of the conformers at $T = 298$ K are given by

$$p_i = \frac{e^{-\Delta G_i/RT}}{1 + \sum_{i=1}^{n} e^{-\Delta G_i/RT}}, \quad \Delta G_i = G_i - G_{st} \quad (8)$$

Results for p_i were used to calculate the energies and enthalpies of the equilibrium mixture of the conformers (Table S2, Supporting Information) and finally applied for calculation of the gaseous enthalpy of formation, $\Delta_f H_m^\circ(g)$, of HMF (see Table 3, last entry). The Mulliken charge distribution of the most stable conformer of 5-hydroxymethylfurfural as calculated using G3MP2 is given in Figure 3.

3.5.2. Calculation of the Enthalpy of Formation of HMF. The enthalpy of formation of HMF, $\Delta_f H_m^\circ$(g, 298 K), was calculated according to the atomization reaction

$$C_6H_6O_3 \rightarrow 6C + 6H + 3O \quad (9)$$

along with the selected isodesmic and bond separation reactions

$$C_6H_6O_3 + \text{ethanol} \rightarrow \text{propanediol-1,2} + \text{2-furancarboxaldehyde [98-01-1]} \quad (10)$$

$$C_6H_6O_3 + \text{ethanol} \rightarrow \text{propanediol-1,2} + \text{3-furancarboxaldehyde [498-60-2]} \quad (11)$$

$$C_6H_6O_3 + 18CH_4 \rightarrow 3H_2O + 12C_2H_6 \quad (12)$$

The results of the calculations are presented in Table S3 (Supporting Information) and Table 3. In all cases, the populations of the conformers of HMF according to eq 8 were taken into consideration for calculating of $\Delta_f H_m^\circ$(g, 298 K). Results calculated from the atomization reaction and from reactions 10−12 for HMF are in good agreement (see Table S2, Supporting Information). Using enthalpies of reactions according to eqs 9−12, calculated by G3MP2, together with the experimental enthalpies of formation, $\Delta_f H_m^\circ$(g, 298.15 K), for methane, ethane, ethanol, propanediol-1,2, 2- and 3-furancarboxaldehyde, and water[24] (see Table S3, Supporting Information), the average theoretical enthalpy of formation of HMF was calculated as $\Delta_f H_m^\circ(g)_{G3MP2} = -(333.9 \pm 2.3)$ kJ·mol^{-1} (Table S2, Supporting Information and Table 3), and this value is in excellent agreement with the experimental result of $\Delta_f H_m^\circ(g) = -(334.2 \pm 1.4)$ kJ·mol^{-1}(see Table 3).

3.5.3. Strength of the Intramolecular Hydrogen Bond in HMF. Our calculations revealed the possibility of intramolecular hydrogen bonding in the most stable conformer of HMF, denoted C1 in Figure 2. Indeed, the distance between the hydrogen of the hydroxyl group and the oxygen in the ring is 2.69 Å, and the Mulliken charges on the hydrogen of the OH group and the furan oxygen are favorable (see Figure 3). For comparison, in 1,2-ethanediol, where the intramolecular hydrogen bond is well-established, a distance of 2.24 Å between the hydrogen of the hydroxyl and the oxygen of the second hydroxyl group was calculated using the same G3MP2 method. Although spectroscopic data[25] can provide qualitative evidence of the presence of intramolecular hydrogen bonding, it has proven difficult to determine the hydrogen-bond strength quantitatively by this approach.[26] Ab initio calculation is one means to determine the hydrogen-bond strength in HMF, which can be defined as the energetic difference between the H-bonded conformer (Figure 4) and an appropriate conformer obtained by rotation of the hydroxyl group by 180° about the C−O single bond with subsequent geometry optimization. Our G3MP2 calculations of the H-bond strength of the conformer C1 performed in this way provided a weak value of 5.9 kJ mol^{-1}. Another simple way to assess the H-bond strength is to consider the enthalpy differences between the H-bonded conformer C1 and non-H-bonded conformers C3−C7, which are also, on average, about 5 kJ mol^{-1} less stable than the hydrogen-bonded

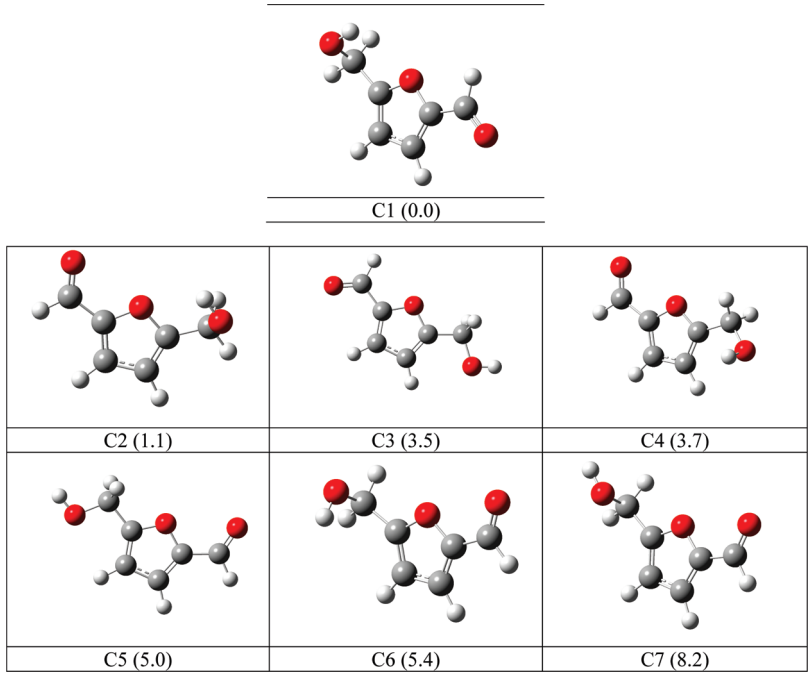

Figure 2. Conformational analysis of 5-hydroxymethylfurfural performed using G3MP2.

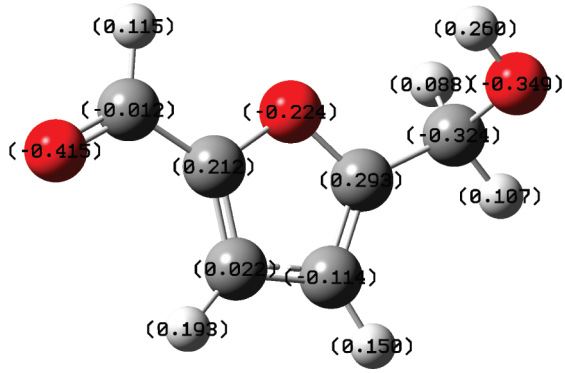

Figure 3. Mulliken charge distribution in 5-hydroxymethylfurfural calculated using G3MP2.

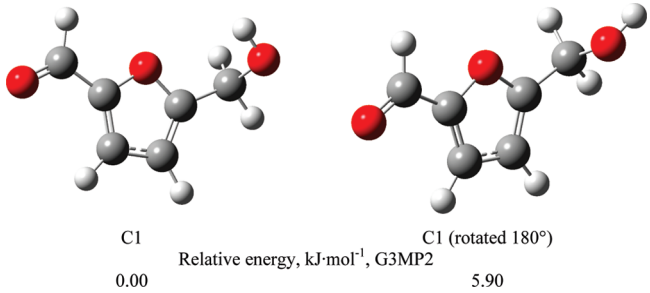

Figure 4. Strength of intramolecular hydrogen bonding in 5-hydroxymethylfurfural calculated using G3MP2.

conformer C1. Thus, a H-bond strength in HMF of about 5 kJ mol^{-1} is predicted using two procedures based on ab initio calculations.

3.5.4. Thermodynamic Analysis of HMF Reactions in the Gas Phase. In general, knowledge of the Gibbs energy, $\Delta_r G^\circ_m$, of any chemical reaction allows for an assessment of the thermodynamic equilibrium constant, K_p, for this reaction in the gaseous phase according to the general equation

$$\Delta_r G^\circ_m = -RT \ln K_p \qquad (13)$$

Table 4. Thermodynamic Functions of the Hydrogenation Reactions R1−R3 (See Figure [1]): Gibbs Energy, $\Delta_r G^\circ_m$, and Reaction Enthalpy, $\Delta_r H^\circ_m$, Calculated Using the B3LYP and G3MP2 Methods

B3LYP/6-311++G(3df,3pd)					
$\Delta_r G^\circ_{m1}$	−13.1	K_{p1}	2.0×10^{2}	$\Delta_r H^\circ_{m1}$	−46.9
$\Delta_r G^\circ_{m2}$	−217.9	K_{p2}	1.5×10^{38}	$\Delta_r H^\circ_{m2}$	−199.8
$\Delta_r G^\circ_{m3}$	−42.5	K_{p3}	2.7×10^{7}	$\Delta_r H^\circ_{m3}$	−115.8
Σ	−273.5			Σ	−362.5
G3MP2					
$\Delta_r G^\circ_{m1}$	−23.0	K_{p1}	1.1×10^{4}	$\Delta_r H^\circ_{m1}$	−254.9
$\Delta_r G^\circ_{m2}$	−206.7	K_{p2}	1.6×10^{34}	$\Delta_r H^\circ_{m2}$	−293.0
$\Delta_r G^\circ_{m3}$	−59.8	K_{p3}	2.9×10^{10}	$\Delta_r H^\circ_{m3}$	−298.5
Σ	−289.5			Σ	−846.4

Table 5. Thermodynamic Functions of the Oxidation Reactions R4−R6 (See Figure [1]): Gibbs Energy, $\Delta_R G^\circ_m$, and Reaction Enthalpy, $\Delta_R H^\circ_m$, Calculated Using the B3LYP and G3MP2 Methods

B3LYP/6-311++G(3df,3pd)					
$\Delta_r G^\circ_{m4}$	−271.4	K_{p4}	3.5×10^{47}	$\Delta_r H^\circ_{m4}$	−57.3
$\Delta_r G^\circ_{m5}$	−292.6	K_{p5}	1.8×10^{51}	$\Delta_r H^\circ_{m5}$	−187.9
$\Delta_r G^\circ_{m6}$	−297.5	K_{p6}	1.3×10^{52}	$\Delta_r H^\circ_{m6}$	−132.5
Σ	−861.5			Σ	−377.8
G3MP2					
$\Delta_r G^\circ_{m4}$	−249.4	K_{p4}	4.6×10^{44}	$\Delta_r H^\circ_{m4}$	−232.4
$\Delta_r G^\circ_{m5}$	−315.7	K_{p5}	2.1×10^{51}	$\Delta_r H^\circ_{m5}$	−315.9
$\Delta_r G^\circ_{m6}$	−320.6	K_{p6}	2.0×10^{52}	$\Delta_r H^\circ_{m6}$	−321.5
Σ	−885.6			Σ	−869.9

If $K_p \geq 1$ as estimated according to eq 13, then the yields of the products should apparently be higher than 50%. In this work, thermodynamic functions of hydrogenation reactions R1−R3 and oxidation reactions R4−R6 (see Figure 1), namely, the Gibbs energy $\Delta_r G^\circ_m$ and the reaction enthalpy, $\Delta_r H^\circ_m$, were calculated using the B3LYP and G3MP2 methods (see Tables 4 and 5). The thermodynamic equilibrium constants in the gaseous phase, K_p, of hydrogenation reactions R1−R3 at 298 K were calculated according to eq 13 and are given in Table 4. As can be seen, the very high values of K_p for all three reactions provide evidence that, at 298 K, the equilibrium of the hydrogenation is completely shifted in the desired direction of

the products. The thermodynamic equilibrium constants in the gaseous phase, K_p, of oxidation reactions R4−R6 at the reference temperature of 298.15 K are also very high (see Table 5). Thus, our calculations of the values of K_p for the rearrangements of HMF in the gaseous phase indicate thermodynamically favorable conditions for both directions of possible utilization: hydrogenation and oxidation. However, these reactions are often carried out in the liquid phase. Hence, the question arises as to how to transfer the results of the ab initio calculations to the liquid state. Thermodynamic equilibrium constants, K_p, calculated for gas-phase reactions R1−R6 (Figure 1, Tables 4 and 5) are related to the thermodynamic constants K_a of these reactions in the liquid phase by the equation

$$K_a = K_p(P_{HMF}/P_{product})P_{H_2/O_2} \quad (14)$$

where P_i, i = H_2, O_2, HMF, or product, represents the appropriate partial vapor pressure of hydrogen, oxygen, 5-hydroxymethylfurfural, or the hydrogenation or oxidation product, respectively, according to reactions R1−R6 (see Figure 1). (P_{H_2/O_2} is always in the gaseous phase.) In fact, the ratio of vapor pressures $P_{HMF}/P_{product}$ does not contribute substantially to eq 14. Therefore, the values of K_p for the gas-phase reactions R1−R6 calculated by the B3LYP and G3MP2 methods (Tables 4 and 5) provide the level of the thermodynamic equilibrium constants K_a in the liquid phase. Thus, it is now also apparent that the similarly high values of K_a for the equilibrium of the HMF rearrangement in the liquid phase are also completely shifted to the desired hydrogenation or oxidation products (see Figure 1). According to our computational studies, we are now able to conclude that all of the HMF reactions considered are thermodynamically very favorable and that high yields can be expected even at ambient temperatures.

The challenge of exploiting HMF-derived molecules as chemical intermediates and fuels thus lies in the provision of efficient engineering technologies that allow for economically competitive production, including the development of highly active and selective catalysts. Some examples in the literature highlight that progress is being made: the catalytic hydrogenation of HMF has been described using different supported catalysts (nickel, cobalt, platinum, palladium, copper, chromium, molybdenum) with dihydrogen.[3,8,27–31] In addition to their potential application as fuels or fuel additives,[3,4,29] hydrogenated derivatives of HMF have been investigated in the manufacture of polymers[11] such as polyesters and polyurethane foams,[32] featuring excellent thermal insulating capabilities, fire resistance, dimensional stability, and structural strength.

Examples of the catalytic oxidation of HMF include the use of oxygen or air in the presence of a base and platinum on a solid support,[33–38] a heterogeneous vanadium-based catalyst in dimethyl sulfoxide (DMSO),[39–42] cobalt acetylacetonate [Co(acac)$_3$] encapsulated in sol−gel silica,[43] and a Co/Mn/Br/Zr catalyst with acetic acid.[44] Oxidized derivatives of HMF can find application as starting materials for the synthesis of antifungal agents, drugs, and ligands;[41,45] building blocks for ligand synthesis;[46] starting material for polyurethanes, polyesters, and polyamides with potentially new properties.[47]

Finally, and perhaps most importantly, biorefinery concepts providing glucose from polymeric renewable resources such as cellulose or starch need to be further developed to reduce the feed prices of the monosaccharide starting material for HMF production, as well as to lessen the food-versus-feed controversy.

4. Conclusions

The purpose of this work was to establish a consistent set of experimental and computed thermochemical quantities for 5-hydroxymethylfurfural and parent compounds. The derived values can be applied for the prediction of the feasibility of HMF utilization processes and for modeling and simulation of the thermochemistry and kinetics of the conversion of 5-hydroxymethylfurfural into bulk intermediates.

Acknowledgment

This work was supported by the German Research Foundation (DFG) priority program SPP 1191, as well as by the Research Training Group 1213 "New Methods for Sustainability in Catalysis and Technique" (DFG).

Supporting Information Available: Auxiliary properties for combustion calorimetry (Table S1), results of the conformational analysis for HMF (Table S2), and total energies at 0 K and enthalpies at 298 K (in Hartree) for the molecules studied in this work and experimental data for compounds used in the thermochemical calculations (Table S3). This information is available free of charge via the Internet at http://pubs.acs.org.

Literature Cited

(1) Gruter, G. J. M. (Furanix Technologies). 5-(Substituted methyl)-2-methylfuran. World Patent WO 2009030510, 2009.

(2) Gruter, G. J. M.; Dautzenberg, F.; Purmova, J. (Avantium International). Method for the Synthesis of Organic Acid Esters of 5-Hydroxymethylfurfural and Their Use. World Patent WO 2007104515, 2007.

(3) Román-Leshkov, B. V. Y.; Barett, C. J.; Liu, Z. Y.; Dumesic, J. A. Phase Modifiers Promote Efficient Production of Hydroxymethylfurfural from Fructose. *Nature* **2007**, *447*, 982–985.

(4) Binder, J. B.; Raines, R. T. Simple Chemical Transformation of Lignocellulosic Biomass into Furans for Fuels and Chemicals. *J. Am. Chem. Soc.* **2009**, *131*, 1979–1985.

(5) Zhao, H.; Holladay, J. E.; Brown, H.; Zhang, Z. C. Metal Chlorides in Ionic Liquid Solvents Convert Sugars to 5-Hydroxymethylfurfural. *Science* **2007**, *316*, 1597–1600.

(6) Zhao, H.; Holladay, J. E.; Zhang, Z. C. (Battelle Memorial Institute). Method for Conversion of Carbohydrates in Ionic Liquids to Hydroxymethylfurfural. World Patent WO 2008019219, 2008.

(7) Yong, G.; Zhang, Y.; Ying, J. Y. Efficient Catalytic System for the Selective Production of 5-Hydroxymethylfurfural from Glucose and Fructose. *Angew. Chem., Int. Ed.* **2008**, *47*, 9345–9348.

(8) Faury, A.; Gaset, A.; Gorrichon, J. P. Réactivité et valorisation chimique de l'hydroxyméthyl-5 furannecarboxaldéhyde-2. *Inf. Chim.* **1981**, *214*, 203–209.

(9) Musau, R. M.; Mnuavu, R. M. The Conversion of 2-Furaldehyde into Some Potentially Useful Bifunctional Derivatives. *Biomass* **1990**, *23*, 275–287.

(10) Gandini, A.; Belgacem, M. N. Furans in Polymer Chemistry. *Prog. Polym. Sci.* **1997**, *22*, 1203–1379.

(11) Moreau, C.; Belgacem, M. N.; Gandini, A. Recent Catalytic Advances in the Chemistry of Substituted Furans from Carbohydrates and in the Ensuing Polymers. *Top. Catal.* **2004**, *27*, 11–30.

(12) Kulikov, D.; Verevkin, S. P.; Heintz, A. Enthalpies of Vaporization of a Series of Linear Aliphatic Alcohols. Experimental Measurements and Application of the ERAS Model for their Prediction. *Fluid Phase Equilib.* **2001**, *192*, 187–202.

(13) Verevkin, S. P. *Experimental Thermodynamics: Measurement of the Thermodynamic Properties of Multiple Phases*; Elsevier: New York, 2005; Vol. 7, Chapter 1, pp6−30.

(14) Emel'yanenko, V. N.; Verevkin, S. P.; Burakova, E. N.; Roganov, G. N.; Gerogieva, M. Thermodynamics of the 4-Pentenoic Acid. *Russ. J. Phys. Chem.* **2008**, *82*, 1–7.

(15) Emel'yanenko, V. N.; Verevkin, S. P.; Heintz, A. The Gaseous Enthalpy of Formation of the Ionic Liquid 1-Butyl-3-methylimidazolium Dicyanoamide from Combustion Calorimetry, Vapor Pressure Measurements, and Ab Initio Calculations. *J. Am. Chem. Soc.* **2007**, *129*, 3930–3937.

(16) Atomic Weights of the Elements. Review 2000. *Pure Appl. Chem.* **2003**, *75*, 683−800.

(17) Hubbard, W. N.; Scott, D. W.; Waddington, G. *Experimental Thermochemistry*; Interscience: New York, 1956; pp 75−127.

(18) Frisch, M. J.; Trucks, G. W.; Schlegel, H. B.; Scuseria, G. E.; Robb, M. A.; Cheeseman, J. R.; Montgomery, J. A., Jr.; Vreven, T.; Kudin, K. N.; Burant, J. C.; Millam, J. M.; Iyengar, S. S.; Tomasi, J.; Barone, V.; Mennucci, B.; Cossi, M.; Scalmani, G.; Rega, N.; Petersson, G. A.; Nakatsuji, H.; Hada, M.; Ehara, M.; Toyota, K.; Fukuda, R.; Hasegawa, J.; Ishida, M.; Nakajima, T.; Honda, Y.; Kitao, O.; Nakai, H.; Klene, M.; Li, X.; Knox, J. E.; Hratchian, H. P.; Cross, J. B.; Bakken, V.; Adamo, C.; Jaramillo, J.; Gomperts, R.; Stratmann, R. E.; Yazyev, O.; Austin, A. J.; Cammi, R.; Pomelli, C.; Ochterski, J. W.; Ayala, P. Y.; Morokuma, K.; Voth, G. A.; Salvador, P.; Dannenberg, J. J.; Zakrzewski, V. G.; Dapprich, S.; Daniels, A. D.; Strain, M. C.; Farkas, O.; Malick, D. K.; Rabuck, A. D.; Raghavachari, K.; Foresman, J. B.; Ortiz, J. V.; Cui, Q.; Baboul, A. G.; Clifford, S.; Cioslowski, J.; Stefanov, B. B.; Liu, G.; Liashenko, A.; Piskorz, P.; Komaromi, I.; Martin, R. L.; Fox, D. J.; Keith, T.; Al-Laham, M. A.; Peng, C. Y.; Nanayakkara, A.; Challacombe, M.; Gill, P. M. W.; Johnson, B.; Chen, W.; Wong, M. W.; Gonzalez, C.; Pople, J. A. *Gaussian 03*, revision B.04; Gaussian, Inc.: Pittsburgh, PA, 2003.

(19) Curtiss, L. A.; Redfern, P. C.; Raghavachari, K.; Rassolov, V.; Pople, J. A. Gaussian-3 Theory Using Reduced Møller−Plesset Order. *J. Chem. Phys.* **1999**, *110*, 4703–4709.

(20) McQuarrie, D. A. *Statistical Mechanics*; Harper & Row: New York, 1976.

(21) Chickos, J. S.; Acree, W. E., Jr. Enthalpies of Vaporization of Organic and Organometallic Compounds.1880−2002. *J. Phys. Chem. Ref. Data* **2003**, *32*, 519–878.

(22) *CODATA Key Values for Thermodynamics*; Hemisphere: New York, 1989.

(23) Middendorp, J. A. Hydroxymethylfurfural. *Recl. Trav. Chim. Pays-Bas Belg.* **1919**, *38*, 1–71.

(24) Pedley, J. P.; Naylor, R. D.; Kirby, S. P. *Thermochemical Data of Organic Compounds*; Chapman and Hall: London, 1986.

(25) Jeffrey, G. A. *An Introduction to Hydrogen Bonding* Oxford University Press: New York, 1997.

(26) Heintz, A.; Kapteina, S.; Verevkin, S. P. Pairwise Substitution Effects and Intramolecular Hydrogen Bond in Nitrophenols and Methylnitrophenols. Thermochemical Measurements and ab Initio Calculations. *J. Phys. Chem. B* **2007**, *111*, 6552–6562.

(27) Utne, T.; Garber, J. D.; Jones, R. E. (Merck & Co., Inc.). Hydrogenation of 5-Hydroxymethyl Furfural. U.S. Patent 3,083,236, 1963.

(28) Schiavo, V.; Descotes, G.; Mentech, J. Catalytic Hydrogenation of 5-Hydroxymethylfurfural in Aqueous Medium. *Bull. Soc. Chim. Fr.* **1991**, *128*, 704–711.

(29) Correia, P. Liquid Biofuels Containing Dihydroxyfuran, Propanol and Its Production Process from Polyols Originated in Agriculture. World Patent WO 2008053284, 2008.

(30) Lilga, M. A.; Hallen, R. T.; Werpy, T. A.; White, J. F.; Holladay, J. E.; Frye, G. J.; Zacher, A. H. (Battelle Memorial Institute). Hydroxymethylfurfural Reduction Methods and Methods of Producing Furandimethanol. U.S. Patent Application 2007287845, 2007.

(31) Huber, G. W.; Chheda, J. N.; Barrett, C. J.; Dumesic, J. A. Production of Liquid Alkanes by Aqueous-Phase Processing of Biomass-Derived Carbohydrates. *Science* **2005**, *308*, 1446–1450.

(32) Pentz, W. J. (Quaker Oats Company). Polyurethanes or Isocyanurates from Alkoxylated Hydroxymethylfuran. U.S. Patent 4,426,460, 1984.

(33) Kröger, M.; Prüsse, U.; Vorlog, K.-E. A New Approach for the Production of 2,5-Furandicarboxylic Acid by in Situ Oxidation of 5-Hydroxymethylfurfural Starting from Fructose. *Top. Catal.* **2000**, *13*, 237–242.

(34) Leupold, E. I.; Wiesner, M.; Schlingmann, M.; Kapp, K. (Hoechst AG). Process for the Oxidation of 5-Hydroxymethylfurfural. European Patent EP 0356703, 1990.

(35) Merat, N.; Verdeguer, P.; Rigal, L.; Gaset, A.; Delmas, M. (Furchim). Process for the Manufacture of Furan-2,5-Dicarboxylic Acid. French Patent FR 2669634, 1992.

(36) Verdeguer, P.; Merat, N.; Gaset, A. Oxydation catalytique du HMF en acide 2,5-furane dicarboxylique. *J. Mol. Catal.* **1993**, *85*, 327–344.

(37) Vinke, P.; v.; Dam, H. E.; van Bekkum, H. Platinum Catalyzed Oxidation of 5-Hydroxymethylfurfural. *Stud. Surf. Sci. Catal.* **1990**, 147–157.

(38) Vinke, P.; v.d.; Pel, W.; van Bekkum, H. On the Oxygen Tolerance of Noble Metal Catalysts in Liquid Phase Alcohol Oxidations. The Influence of the Support on Catalyst Deactivation. *Stud. Surf. Sci. Catal.* **1991**, 385–394.

(39) Halliday, G. A.; Young, R. J.; Grushin, V. V. One-Pot, Two-Step, Practical Catalytic Synthesis of 2,5-Diformylfuran from Fructose. *Org. Lett.* **2003**, *5*, 2003−−2005.

(40) Carlini, C.; Patrono, P.; Galletti, A. M. R.; Sbrana, G.; Zima, V. Selective Oxidation of 5-Hydroxymethyl-2-furaldehyde to Furan-2,5-dicarboxaldehyde by Catalytic Systems Based on Vanadyl Phosphate. *Appl. Catal. A: Gen.* **2005**, *289*, 197–204.

(41) Grushin, V.; Herron, N.; Halliday, G. A. (Dupont). Process for Preparing 2,5-Diformylfuran from Carbohydrates. World Patent WO 03024947, 2003.

(42) Lilga, M. A.; Hallen, R. T.; White, J. F.; Frye, G. J. (Battelle Memorial Institute). Hydroxymethyl Furfural Oxidation Methods. U.S. Patent Application 20080103318, 2008.

(43) Ribeiro, M. L.; Schuchardt, U. Cooperative Effect of Cobalt Acetylacetonate and Silica in the Catalytic Cyclization and Oxidation of Fructose to 2,5-Furandicarboxylic Acid. *Catal. Commun.* **2003**, *4*, 83–86.

(44) Partenheimer, W.; Grushin, V. V. Synthesis of 2,5-Diformylfuran and Furan-2,5-Dicarboxylic Acid by Catalytic Air Oxidation of 5-Hydroxymethylfurfural. Unexpectedly Selective Aerobic Oxidation of Benzyl Alcohol to Benzaldehyde with Metal/Bromide Catalysts. *Adv. Synth. Catal.* **2001**, *343*, 102–111.

(45) Del Poeta, M.; Schell, W. A.; Dykstra, C. C.; Jones, S.; Tidwell, R. R.; Czarny, A.; Bajic, M.; Kumar, A.; Boykin, D.; Perfect, J. R. Structure−in Vitro Activity Relationships of Pentamidine Analogues and Dication-Substituted Bis-Benzimidazoles as New Antifungal Agents. *Antimicrob. Agents Chemother.* **1998**, *42*, 2495–2502.

(46) Chmielewski, P. J.; Latos-Grazynski, L.; Olmstead, M. M.; Balch, A. L. Nickel Complexes of 21-Oxaporphyrin and 21,23-Dioxaporphyrin. *Chem.−Eur. J.* **1997**, *3*, 268–278.

(47) Werpy, T., Petersen, G., eds. *Top Value Added Chemicals from Biomass. Vol. 1: Results of Screening for Potential Candidates from Sugars and Synthesis Gas*, National Renewable Energy Laboratory: Golden, CO, 2004.

Received for review June 23, 2009
Revised manuscript received August 14, 2009
Accepted August 26, 2009

IE901012G